

ElAM: A computer program for the analysis and representation of anisotropic elastic properties ☆

Arnaud Marmier^{a,*}, Zoe A.D. Lethbridge^b, Richard I. Walton^b, Christopher W. Smith^a,
Stephen C. Parker^c, Kenneth E. Evans^a

^a College of Engineering, Mathematics and Physical Sciences, University of Exeter, Exeter, EX4 4QF, UK

^b Department of Chemistry, University of Warwick, Coventry, CV4 7AL, UK

^c Department of Chemistry, University of Bath, Bath, BA2 7AY, UK

ARTICLE INFO

Article history:

Received 11 September 2009

Received in revised form 6 August 2010

Accepted 23 August 2010

Available online 22 September 2010

Keywords:

Elastic properties

Anisotropy

Visualisation

Database

ABSTRACT

The continuum theory of elasticity has been used for more than a century and has applications in many fields of science and engineering. It is very robust, well understood and mathematically elegant. In the isotropic case elastic properties are easily represented, but for non-isotropic materials, even in the simple cubic symmetry, it can be difficult to visualise how properties such as Young's modulus or Poisson's ratio vary with stress/strain orientation. The ElAM (Elastic Anisotropy Measures) code carries out the required tensorial operations (inversion, rotation, diagonalisation) and creates 3D models of an elastic property's anisotropy. It can also produce 2D cuts in any given plane, compute averages following diverse schemes and query a database of elastic constants to support meta-analyses.

Program summary

Program title: ElAM1.0

Catalogue identifier: AEHB_v1_0

Program summary URL: http://cpc.cs.qub.ac.uk/summaries/AEHB_v1_0.html

Program obtainable from: CPC Program Library, Queen's University, Belfast, N. Ireland

Licensing provisions: Standard CPC licence, <http://cpc.cs.qub.ac.uk/licence/licence.html>

No. of lines in distributed program, including test data, etc.: 43 848

No. of bytes in distributed program, including test data, etc.: 2 498 882

Distribution format: tar.gz

Programming language: Fortran90

Computer: Any

Operating system: Linux, Windows (XP, Vista)

RAM: Depends chiefly on the size of the arrays representing elastic properties in 3D

Classification: 7.7

Nature of problem: Representation of elastic moduli and ratios, and of wave velocities, in 3D; automatic discovery of unusual elastic properties.

Solution method: Stiffness matrix (6×6) inversion and conversion to compliance tensor ($3 \times 3 \times 3 \times 3$), tensor rotation, dynamic matrix diagonalisation, simple optimisation, postscript and VRML output preparation.

Running time: Dependent on angular accuracy and size of elastic constant database (from a few seconds to a few hours). The tests provided take from a few seconds for test0 to approximately 1 hour for test4.

© 2010 Elsevier B.V. All rights reserved.

1. Introduction

In materials science, engineering or physics, the theory of elasticity is typical undergraduate fare: it has been around for a very long time, works very well, is linear, and is really not very complicated. It is also used to introduce interesting mathematical objects and, more

☆ This paper and its associated computer program are available via the Computer Physics Communications homepage on ScienceDirect (<http://www.sciencedirect.com/science/journal/00104655>).

* Corresponding author.

E-mail address: a.s.h.marmier@exeter.ac.uk (A. Marmier).

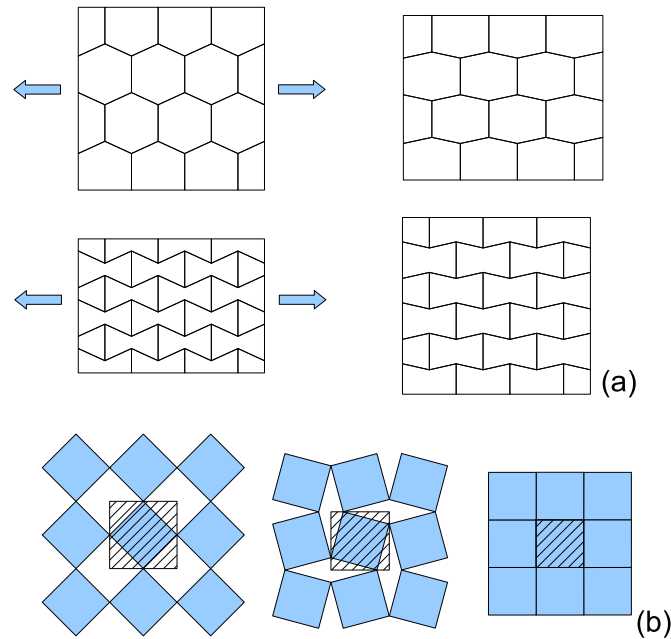


Fig. 1. (a) 2D structure with positive (top) and negative (bottom) Poisson's ratio; (b) 2D illustration of one mechanism of NTE, increasing thermal agitation of linked, rigid squares reduces total area.

often than not, students in physical sciences discover the magic of tensors in a course on crystalline elasticity. Despite its familiarity, this old theory has been rejuvenated in the last two decades as materials with odd elastic properties have been discovered and investigated.

When a sample is stretched, it usually gets thinner, and materials behaving so familiarly have a positive Poisson's ratio. While negative Poisson's ratios (hereby NPR) are not theoretically prohibited, materials exhibiting them have only been produced or recognised recently. It is easy to convince oneself of the theoretical possibility of NPR by considering the now canonical re-entrant honeycomb structure (see Fig. 1a).

The first NPR material to find wide recognition was of the re-entrant type, a polymeric foam which had been compressed to generate concavity [1]. Since then, many other materials have been observed or postulated, and it has been observed that many crystals exhibit NPR, including many cubic metals [2]. This last result is certainly striking, but it is even more surprising that it was only established in 1998.

Some even rarer materials exhibit another unusual elastic property: when subjected to hydrostatic (isotropic) pressure, they expand in one direction [3,4]. This property is referred to as Negative Linear Compressibility (NLC). It has been observed in only 14 materials.

Finally, and even if not yet implemented in the present code, thermoelastic properties can also be surprising. Negative Thermal Expansion (NTE), where a material contracts in one, two or three directions as temperature increases, has received a lot of interest [5] due to possible technological applications such as dental fillings that expand with the tooth or beams that do not change shape at all with temperature. Many mechanisms can generate it, and one of the simplest is illustrated in Fig. 1b.

One of the problems with the full anisotropic elasticity theory is that, while beautifully symmetric and compact, it is not especially visualisable. First, the link between the interesting properties (moduli and ratios) and the available data (usually the stiffness matrix) is not evident (it can be slightly more direct with the compliance matrix but only in the case of distortions on the principal axes). Worst, for distortions in less symmetric directions, the calculations are too taxing to be carried by hand on a regular basis, and even exceed the potentiality of spreadsheet automation (for typical users). On the other hand, it is well adapted to programming as it is essentially linear algebra, for which many efficient algorithms are available.

It is therefore very surprising to note that there is no easily available code that would transpose the somehow abstract numbers of the stiffness matrix into 3D or 2D representations of elastic properties. 2D figures of Poisson's ratio have been published, but it is almost certain that they have been produced with spreadsheets (limitation to principal planes and perpendicular strains). There are also examples in the literature of 3D plots for the Young's modulus (by far the simplest property), but the authors do not indicate how they were produced [6,7].

There lies the main motivation behind the present work: to offer a free, easy to use program, EIAM (Elastic Anisotropy Measures), capable of representing various elastic properties in any direction, for any crystal symmetry. A secondary goal is to allow the code to automatically query a database of elastic constants (as can be found in reviews such as [8] or [9]), in order to systematically investigate the occurrence of bizarre properties or possible correlations and trends.

The Methodology section first introduces the tensorial formalism behind the crystalline theory of elasticity and establishes the convention used for angles. It also presents various averaging schemes. It then details the algorithm used to compute the principal properties, namely tensor rotation and dynamical matrix diagonalisation. The slightly more subtle case of the Poisson's ratio and shear modulus, which requires some optimisation if the results are to be visualisable in 3D, are treated separately.

We then describe the keywords and input files and present four cases studies, which illustrate some of EIAM capabilities. The first two focus on the visualisation aspect and show that the cubic symmetry can still surprise and that some materials (cristobalite, lanthanum niobate) have truly astonishing elastic properties. The last two examples display the database facilities by revisiting the NLC problem (identifying two new materials), and offering insight on how various definitions of elastic anisotropy are related.

2. Methodology

2.1. Elasticity theory

At its most basic, the theory of elasticity linearly relates stresses to strains. This section introduces the various quantities, but without delving into subtleties. The interested reader is invited to consult standards text [10,11].

The stress describes the surface forces acting on volume element in a continuum. It can be represented by a 2nd order tensor, with 6 independent coordinates.

The strain describes the state of deformation of a solid body. It can also be represented by a 2nd order tensor, with 6 independent coordinates.

The stiffness tensor expresses the stress tensor in terms of the strain tensor:

$$\sigma_{ij} = C_{ijkl} \varepsilon_{kl}. \quad (1)$$

It is a property of the crystal, a tensor of 4th order, and its coordinates depend on the choice of axis. Eq. (1) is the generalised Hooke's law.

The compliance tensor is the inverse of the stiffness tensor and interprets the strain tensor in terms of the stress tensor:

$$\varepsilon_{ij} = S_{ijkl} \sigma_{kl}. \quad (2)$$

Young's modulus, or modulus of elasticity, is defined as the ratio of normal stress to linear normal strain (both in the direction of applied load).

The shear modulus, or modulus of rigidity, is defined as the ratio of shear stress to linear shear strain.

Poisson's ratio is defined as the ratio of transverse strain (normal to the applied load), to axial strain (in the direction of the applied load).

When the crystal is submitted to hydrostatic pressure, the linear compressibility is the ratio of the induced stretch, along a given line, by the pressure. Except in crystal of cubic symmetry, where compressibility is isotropic, it depends on the direction of the line.

The long wavelength acoustic phonons, those which originate from translation at the Γ -point, correspond to strains. It is therefore possible to establish a parallel [12] between the atomistic (force constants, dynamical matrix) and continuum descriptions (stiffnesses, Christoffel equation). Out of these three acoustic waves, one is longitudinal, the other two are transverse.

Due to translational and rotational symmetries, the number of independent coordinates of the 4th order tensor reduces to 21 – from 81 – for the least symmetric case. Crystals (and more generally 3D periodic structures or space groups) can be grouped into 7 crystal systems, and the associated symmetries reduce the number of independent components for the 4th order tensors further: triclinic (21), monoclinic (15), orthorhombic (9), trigonal (7), tetragonal (5), hexagonal (5) and cubic (3).

Six components are sufficient to describe stress and strain. A scheme due to Voigt [13] uses this fact and replaces the cumbersome 2nd and 4th order tensors in a 3 dimension vector space by vectors and matrices in a 6 dimension vector space.

Tensor notation	11	22	33	23, 32	31, 13	12, 21	
Voigt's notation	1	2	3	4	5	6	(3)

These transformation rules apply directly for stress and stiffness, but the use of corrective coefficient is required for strain and compliances:

$$\begin{aligned} \varepsilon_{ii} &= \varepsilon_p, & S_{ijkl} &= S_{pq} \text{ if } p \text{ and } q \text{ are } 1, 2, 3 \text{ only.} \\ \varepsilon_{ij} &= \frac{1}{2} \varepsilon_p \text{ if } i \text{ and } j \text{ are different} & S_{ijkl} &= \frac{1}{2} S_{pq} \text{ if either } p \text{ or } q \text{ are } 4, 5, 6 \text{ (and the other is } 1, 2 \text{ or } 3). \\ S_{ijkl} &= \frac{1}{4} S_{pq} \text{ if } p \text{ and } q \text{ are } 4, 5, 6 \text{ only.} \end{aligned} \quad (4)$$

2.2. Tensor rotation, Euler angles

A fourth order tensor transforms in a new basis set following the rule

$$T'_{\alpha\beta\gamma\delta} = r_{\alpha i} r_{\beta j} r_{\gamma k} r_{\delta l} T_{ijkl}, \quad (5)$$

where Einstein's summation rule is adopted and where the $r_{\alpha i}$ are the components of the rotation matrix (or direction cosines). They are expressed as the coordinates of the new basis set vectors in the old framework.

A direction in Cartesian space, corresponding to an elastically significant distortion, for instance uniaxial stress or response to isotropic pressure, can be represented as a point on the unit sphere (unit vector), and advantageously by two angles. We choose it to be the first unit vector in the new basis set, a . It is fully characterised by the angles $\theta(0, \pi)$ and $\phi(0, 2\pi)$, as illustrated in Fig. 2. The determination of some elastic properties (shear modulus, Poisson's ratio) requires another, perpendicular, direction. This is defined by another unit vector, b , perpendicular to the first, and characterised by the angle $\chi(0, 2\pi)$.

The coordinates of the two vectors are

$$a = \begin{pmatrix} \sin \theta \cos \varphi \\ \sin \theta \sin \varphi \\ \cos \theta \end{pmatrix}, \quad \text{and} \quad b = \begin{pmatrix} \cos \theta \cos \varphi \cos \chi - \sin \theta \sin \chi \\ \cos \theta \sin \varphi \cos \chi + \cos \theta \sin \chi \\ -\sin \theta \cos \chi \end{pmatrix}. \quad (6)$$

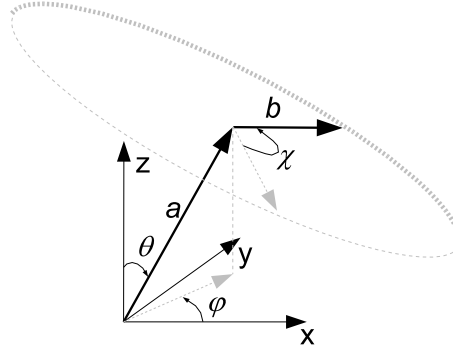


Fig. 2. Definitions of angles used to describe directions in EIAM.

By definition, the components of the first two columns of the rotation matrix are the coordinates of a and b . This is sufficient to obtain all the components of the fourth order in the subvectorial space defined by directions 1 and 2, for instance:

$$S'_{12} = S'_{1122} = r_{1i}r_{1j}r_{2k}r_{2l}S_{ijkl} = a_i a_j b_k b_l S_{ijkl}, \quad \text{and} \quad S'_{66} = S'_{1212} = r_{1i}r_{2j}r_{1k}r_{2l}S_{ijkl} = a_i b_j a_k b_l S_{ijkl}. \quad (7)$$

But by scanning θ , ϕ , and χ over the unit sphere, we can access all the components without having to take into account the third unit vector.

2.3. Averaging schemes

Traditionally, and for ease of manipulation, the elastic properties of an anisotropic material have been replaced by those of an “equivalent” isotropic material. These processes of averaging are especially important to treat materials consisting of crystalline grains of random orientation. There are four main schemes: Voigt [13], Reuss [14], Hill [15], and direct.

The Voigt averaging scheme is based on the stiffness matrix (assuming a given uniform strain) and the bulk modulus K and the shear modulus G are given by

$$K_V = \frac{A + 2B}{3}, \quad G_V = \frac{A - B + 3C}{5}, \quad (8)$$

where

$$A = \frac{C_{11} + C_{22} + C_{33}}{3}, \quad B = \frac{C_{23} + C_{13} + C_{12}}{3}, \quad C = \frac{C_{44} + C_{55} + C_{66}}{3}. \quad (9)$$

Conversely, the Reuss averaging scheme is based on the compliance matrix (assuming a given uniform stress) and:

$$K_R = \frac{1}{3a + 6b}, \quad G_R = \frac{5}{4a - 4b + 3c}, \quad (10)$$

where

$$a = \frac{S_{11} + S_{22} + S_{33}}{3}, \quad b = \frac{S_{23} + S_{13} + S_{12}}{3}, \quad c = \frac{S_{44} + S_{55} + S_{66}}{3}. \quad (11)$$

In both cases, the Young's modulus E and the Poisson's ratio ν are given by

$$E = \left(\frac{1}{3G} + \frac{1}{9K} \right)^{-1}, \quad \nu = \frac{1}{2} \left(1 - \frac{3G}{3K + G} \right). \quad (12)$$

The Hill average is the arithmetic average of the Voigt and Reuss values.

The direct averaging scheme is non-analytical and based on a numerical average of the calculated properties, it converges slowly with the mesh accuracy.

2.4. Simple properties: Young's modulus and linear compressibility

Some properties can be simply expressed in terms of the compliance matrix.

The Young's modulus can be obtained by using a purely normal stress in Eq. (2) in its vector form and is given by

$$E(\theta, \varphi) = \frac{1}{S'_{11}(\theta, \varphi)} = \frac{1}{a_i a_j a_k a_l S_{ijkl}}. \quad (13)$$

The linear compressibility follows a slightly different scheme but is even simpler to compute. It is obtained by applying an isotropic stress (corresponding to pressure p) in tensor form, so that $\varepsilon_{ij} = -p S_{ijkk}$ and by considering that the extension in direction a is $\varepsilon_{ij} a_i a_j$, and that therefore

$$\beta(\theta, \varphi) = S_{ijkk} a_i a_j. \quad (14)$$

2.5. Shear modulus and Poisson's ratio: optimisation

Other properties depends on two directions (if perpendicular this corresponds to 3 angles), which makes them difficult to represent graphically. A convenient possibility is then to consider three representations: minimum, average and maximum. For each θ and ϕ , the angle χ is scanned and the minimum, average and maximum values are recorded for this direction.

The shear ratio is obtained by applying a pure shear stress in the vector form of Eq. (2) and results in

$$G(\theta, \varphi, \chi) = \frac{1}{4S'_{66}(\theta, \varphi, \chi)}. \quad (15)$$

Poisson's ratio can be obtained by using a purely normal stress in Eq. (2) in its vector form and is given by

$$\nu(\theta, \varphi, \chi) = -\frac{S'_{12}(\theta, \varphi, \chi)}{S'_{11}(\theta, \varphi)} = -\frac{a_i a_j b_k b_l S_{ijkl}}{a_i a_j a_k a_l S_{ijkl}}. \quad (16)$$

2.6. Sound velocities: diagonalisation

The dynamic matrix M , which describes the vibrational modes (phonons) in a crystal can be written in terms of the stiffness tensor (see for instance [12])

$$M_{ik} = C_{ijkl} k_j k_l, \quad (17)$$

where $k(k_x, k_y, k_z)$ is the wave vector (coordinates).

The dynamic matrix can be diagonalised, and its eigenvalues w are the square of the frequencies. From the $w(\mathbf{k})$ dependence, we can extract the sound wave velocities.

3. Code structure

The source code is written in Fortran90, makes use of modules and is divided, somehow artificially, in 6 files: `elasticcalculations.f90`, `main.f90`, `modules.f90`, `ouvrir.f90`, `printps.f90` and `system.f90`. `main.f90` contains the main program, which controls the scanning loops and the calls to reading, calculating, and writing procedures. `elasticcalculations.f90` contains procedures to calculate various elastic properties. These are called from `main.f90`, and make uses of linear algebra subroutines from `system.f90`. This last file contains diagonalisation subroutines from J. Kopp [16], and matrix inversion routines from T. Pang [17]. The subroutine in `ouvrir.f90` interprets the input files. The procedures in `printps.f90` deal with the creation of postscript output files, and are called by `main.f90`. Finally, `modules.f90` contains not only various modules used for data transfer between procedures, but also the `vrml` module, which creates the `vrml` output files.

4. Operation and case studies

This section introduces various ELAM input files, discusses parameters, and displays some of the results. It is hoped that the following examples will prove sufficiently explanatory for most users. The full list of keywords is given in [Appendix A](#).

4.1. Installation

The code is distributed as a .rar file, which uncompresses into several directories: `source`, `examples`, `doc` and `bin`.

The `bin` directory contains a precompiled win32 executable for direct uses by windows user, and an accompanying .bat for direct execution.

The `doc` directory contains a copy of this article, and the `examples` directory contains the examples input and database files mentioned in Section 4.2 and onward.

Compilation in the `source` directory consist of a straightforward `g95.exe -o ELAM.exe *.f90` (with the gnu fortran 95 compiler for instance). The code has been developed under a windows platform, and compiles under Compaq Fortran and Silversfrost FTN95. It has also been tested with gnu g95.

For convenience under windows, the main input file must be called `input.txt`, but scripts can of course be used to allow command line or right-button control. In a directory containing an `input.txt` file, the code will run by executing `ELAM.exe`. The name for the output is controlled within the input file, see next section.

4.2. Direct mode: basic operations

One of the simplest input files is given in [Ex. 1](#). The first line sets the crystal system (symmetry), the second line contains the corresponding stiffness constants, in the order given by the Landolt–Börnstein tables (C_{11} , C_{44} , C_{12} for cubic, see [Appendix A](#) for other crystal systems). The third line asks for Young's modulus to be graphically represented, and the last line finishes the input (`stop` must be present). The program would still be running in the absence of a property requirement. The order of the command is unimportant, with the obvious exception that if a keyword requires numerical values, these must be in the line immediately following it.

As is, this input produces two output files, `ELAM.log` and `ELAM_young.vrml`. The first file is a text summary of the calculations. It starts with the stiffness and compliance matrices, which is useful to check that the order of elastic constants was correct. It then recalls the meshing parameters and finally summarises the elastic properties in terms of averages, minimum/maximum values and their directions. The second file is in VRML (virtual reality modelling language) format and can be visualised and explored with a VRML capable browser. A screen copy is shown in [Fig. 3](#).

```
cubi
 12.20 4.46 9.20
young
stop
```

Ex. 1. Basic EIAM input for Young's modulus of silver.

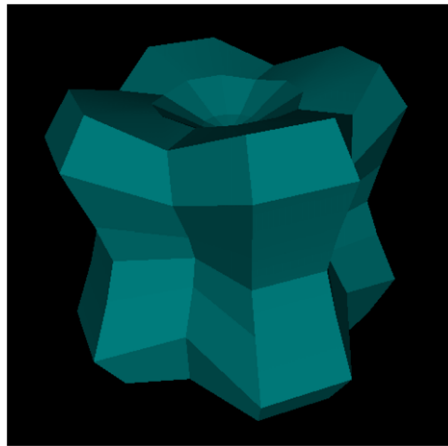


Fig. 3. 3D representation of Young's modulus of silver, using default setup.

```
Title
Silver fcc
output
Ag_fcc
cubi
 12.20 4.46 9.20
thet
200
phi
200
3dth
99
3dph
99
young
3daxes
color_bg
 1. 1. 1.
Stop
```

Ex. 2. Improved EIAM input for Young's modulus of silver, with title, named output, finer angle mesh, white background and axes.

Fig. 3 is not an especially good figure, and for many reasons. In fact, the previous input makes use of many default values, which are perfectly fine to obtain averages and quick indications in the .log files, but lack detail to produce good figures. This can be improved, as in Ex. 2 and the resulting Fig. 4. The first four lines give a title and an output root name. While the title is relatively unimportant, the output root name eases the organisation of files, now called Ag_fcc.log and Ag_fcc_young.vrml. The main difference with Ex. 1 is the refinement of the angular scanning steps: thet and phi control the steps for the calculations of optimum values and average, while 3dth and 3dph define the grid used for the graphical representation. The default values for these are 24, 24, 12 and 12. The 3daxes keyword facilitates orientation by adding arrows and labels for the three Cartesian axes. Finally, the background colour is changed to white with the color_bg keyword. Generally speaking, colour is coded in EIAM with four values (0. to 1.), red, green, blue, and transparency. Transparency being meaningless for the background, it is ignored in that case.

The other property codes are shear, poisson, compress and sound. The symmetry codes are self explanatory and are cubi, hexa, tetr, trig, orth, mono and tric. Each must be followed by a line containing the appropriate number of elastic constant values, 3 for cubi, 5 for hexa, 7 for tetr and trig, 9 for orth, 13 for mono and 21 for tric.

By default, the code interprets the elastic constants following the symmetry keyword as being components of the stiffness matrix. In order to force them to be components of the compliance matrix, one has to add the compli keyword to the input. It is also possible to input the elastic constant directly in 6×6 matrix form, following the keyword C or S (note the capital).

This type of input file is sufficient to explore the elastic properties of a given materials and can already shed light on some interesting phenomena.

4.3. Case study 1: Poisson's ratio of cubic crystals

In 1998, Baughman et al. did show that around two thirds of cubic metals (and alloys) do have negative poisson's ratios, in the (110) direction. Previously, this property had been considered very rare. Figs. 5a and 5b display screen copies of the VRML representation of Poisson's ratio for two cubic metals, cesium and aluminium.

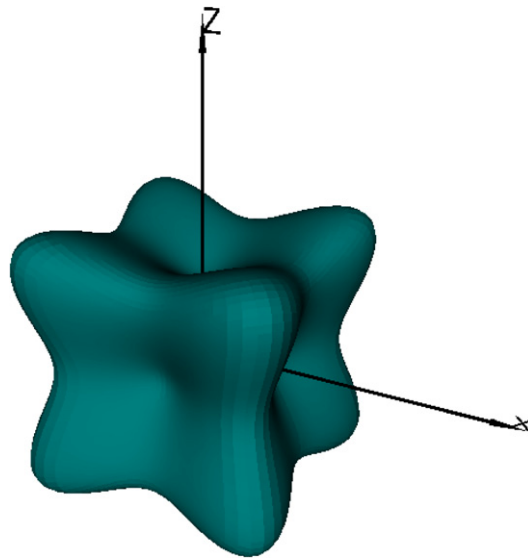


Fig. 4. Improved 3D representation of Young's modulus of silver, with finer angle mesh, white background and axes.

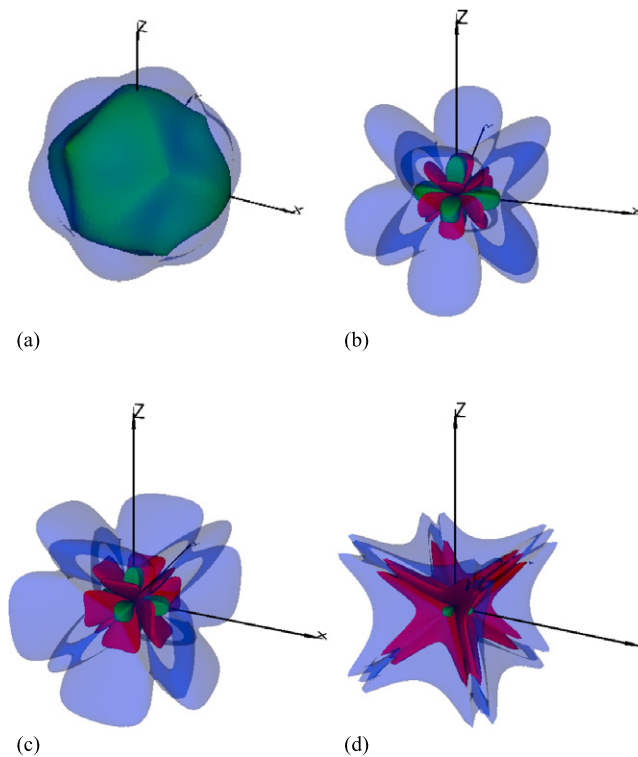


Fig. 5. 3D representation of Poisson's ratio for aluminium (a), cesium (b), AuCd alloy (c) and InTi alloy (d); maximum (blue), minimum positive (green) and minimum negative (red). (For interpretation of the references to colour in this figure legend, the reader is referred to the web version of this article.)

The default ELAM colour convention (transparent blue, maximum; green, minimum if positive, red, minimum when negative) makes it clear that these two metals have different elastic behaviour. Not only does aluminium appear much more isotropic, it also does not show any sign of auxeticity, which is confirmed by the numerical summary in the `.log` file. The convoluted shape for cesium is very interesting as it shows auxeticity, but also because it strongly hints that a visual inspection of this sort, even without the colour scheme could have identified negative Poisson's ratio in cubic metals a lot earlier than 1998.

The humble cubic symmetry is not without surprises, and the story does not stop here. From simple calculations, it was assumed that the extrema of Poisson's ratio for the cubic symmetry were along the $[110]$ directions and permutations (for instance see [2]). If we consider the AuCd alloy in Fig. 5c, we can see that the negative minimum surface is concave at $[110]$, and that therefore this direction is not the one of minimum Poisson's ratio. Recent analytic calculations [18,19] have tackled this problem and pushed it even further, and shown that in some rare cases, the optima can occur in directions around $[111]$. Once again, this peculiarity (referred to as the "Ting & Chen effect") could have been discovered much earlier, tipped off by graphical representations, such as Figs. 5d and 6d for InTi alloy (27% Ti).

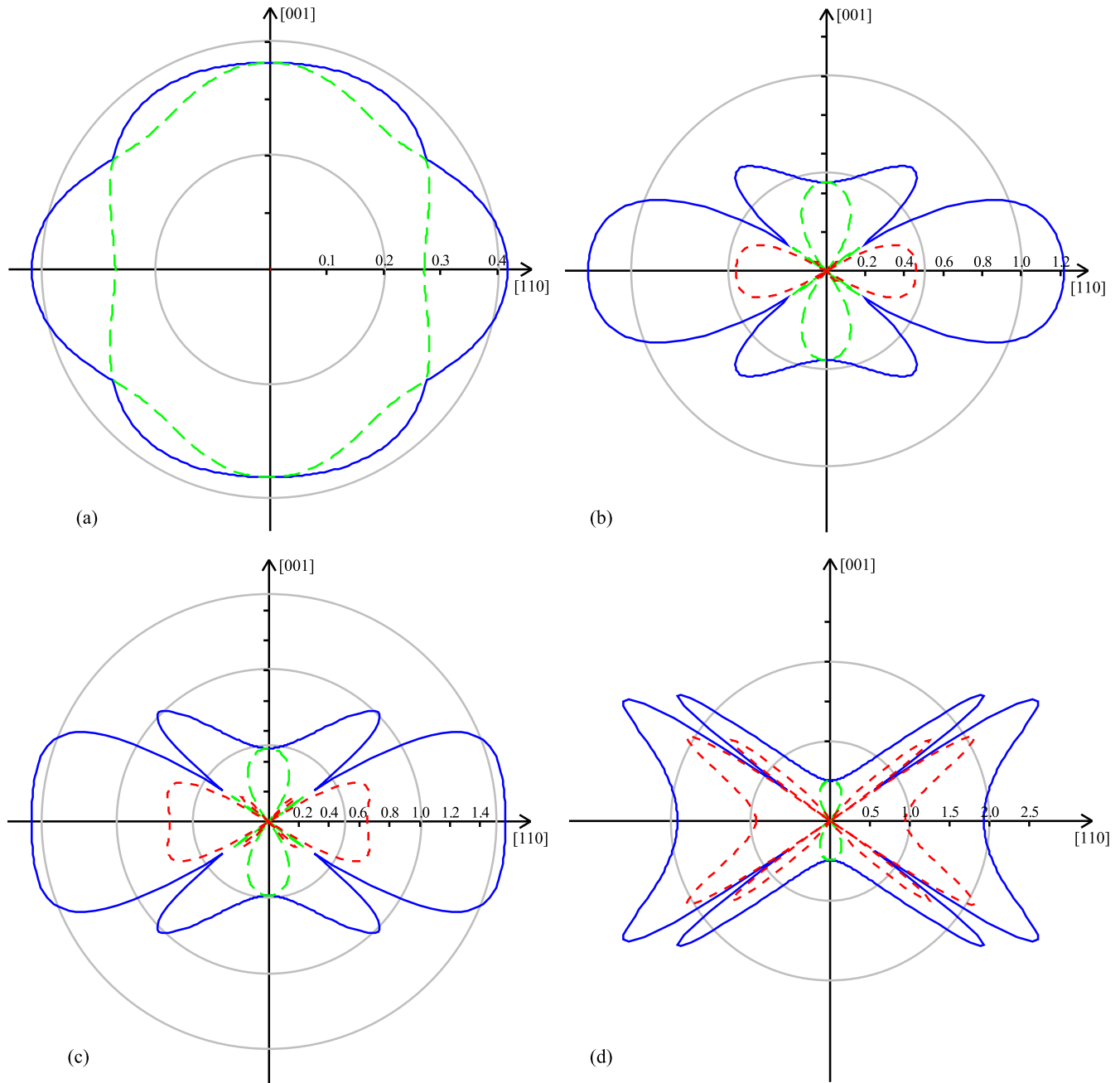


Fig. 6. 2D representation of Poisson's ratio in the (-110) plane for aluminium (a), cesium (b), AuCd alloy (c) and InTi alloy (d); maximum (blue), minimum positive (green) and minimum negative (red). (For interpretation of the references to colour in this figure legend, the reader is referred to the web version of this article.)

4.4. Fine tuning and 2D graphics

As previously mentioned, the simplest properties are easy to represent, and a two-colour scheme is enough. The shear modulus and Poisson's ratio are more complex, with maximum, minimum and average surfaces. EIAM produces all four surfaces in a single VRML file, which could lead to overly rich 3D models. Control over which surfaces are represented is done by using the colour options. By default, the average surface colour is fully transparent and only maximum and minimum appear, minimum following the red/negative, green/positive convention, and maximum being blue and semi-transparent (to reveal the minimum surface underneath). The colour options are `color_bg`, `color_axis`, `color_pos`, `color_neg`, `color_max`, `color_minp`, `color_minn`, `color_aven`, and `color_avep`. They are followed by a line containing RGB numbers, and, with the exception of the first two, a transparency number (0 –opaque– to 1 –transparent–).

It is also possible to plot sections of the curves, in postscript format. The principles are very similar to those of the 3D curves. Whether a property is plotted or not is controlled by the following keywords: `2dyoun`, `2dshea`, `2dpois`, `2dcomp` and `2dsoun`. The plane in which the section is cut is defined by either `plane_xy` followed by a line containing the miller indices, or by `plane_an` followed by two angles defining the unit vector perpendicular to the plane. Other related keywords are of the type `2dyoun_tick` and `2dyoun_circ`; they control the presence of ticks on the axes or of circles to guide the eyes (see Ex. 3 and Fig. 6).


```

...
2dpoisson
2dpois_ticks
.1
2dpois_circle
.2
2dpois_scale
.1
2dshear
2dcompressi
2dyoung
2dsound
plane_xyz
1 0 1
2dtitlex
[110]
2dtitley
[001]
stop

```

Ex. 3. Use of 2D keywords for postscript production, see Fig. 6.

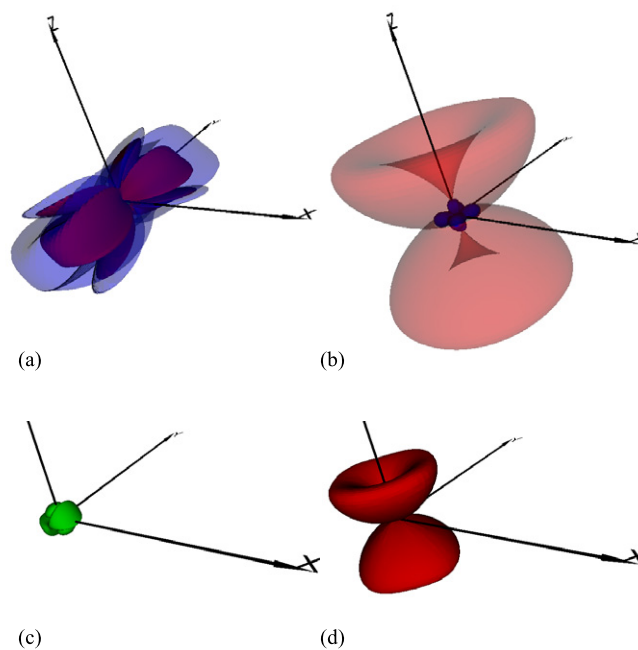


Fig. 7. 3D representation of Poisson's ratio for lanthanum niobate (a, c) and α -cristobalite (b, d). The top figures (a, b) show the maximum and minimum curves for each direction, while the bottom ones (c, d) show the rotationally averaged value. The scale, indicated by the length of the axes, is conserved for each material. The standard colour convention is used (note the, forced, reverse in transparency – red – in b). (For interpretation of the references to colour in this figure legend, the reader is referred to the web version of this article.)

```

...
color_max
0.0 .8 0.
Color_minp
.0 .8 .0 .5
color_minn
.8 .0 .0 .5
stop

```

Ex. 4. Use of colour keywords for transparency reversal.

4.5. Case study 2: extreme crystalline auxeticity

Monoclinic lanthanum niobate is remarkable for being one of few materials exhibiting negative linear compressibility, but it is has also one of the lowest observed Poisson's ratio (-3.01). It also has a very large maximum (3.96), interestingly in the same direction, along the y axis (see Fig. 7a). α -cristobalite, a SiO_2 polymorph, is also an auxetic crystal, as can be seen from Fig. 7b. The extreme values are more modest, at $.10$ and $-.51$, but for almost all directions, the absolute value for the minimum is larger than for the maximum (the reverse in transparency in Fig. 7b was achieved with the EIAM input from Ex. 4).

Both these crystals show extreme auxetic behaviour, yet their properties are strikingly different. Figs. 7c and 7d display the average Poisson's ratio (using input shown in Ex. 5). This value gives an indication of whether the section perpendicular to the stretch increases

```

Title
xtobal
tetr
59.4 42.4 67.2 25.7 3.8 -4.4 0.0
...
poisson
3daxes
color_bg
1. 1. 1.
Color_max
0. 0. .8 1.
Color_minp
.0 .8 .0 1.
Color_minn
.8 .0 .0 1.
Color_avep
.0 .8 .0 0.
Color_aven
.8 .0 .0 0.
Stop

```

Ex. 5. Use of colour keywords to reveal average curves (α -cristobalite).

```

Title
TST_DATABASE
database
exampledb.txt
data_prop 7
110 120 304 310 320 410 420
stop.

```

Ex. 6. Typical database mode input file.

```

Cristoballite C 5 59.4 42.4 67.2 25.7 3.8 -4.4 0.0
AuCd_Alloy C 7 110.8 40.7 104.9
Ag_FCC C 7 122 45.5 92.0
Cd_HCP C 6 114.1 49.9 19.0 41.0 40.3
Aluminium_pentaiodate_sexahydrate C 6 42.9 38.7 16 15.7 21.9
stop.

```

Ex. 7. Database file.

or decreases in area. It can be that while for α -cristobalite, stretches in any direction results in increasing section area, lanthanum niobate follows a much more normal pattern as the section area decreases for any stretch. Both materials are certainly interesting, but would have different applications.

4.6. Database mode

This mode is geared towards the systematic discovery of unusual elastic properties. It does not use graphical representation; although the graphical keyword discussed previously can still be present, they will be ignored. The database mode requires an additional file, containing a list of materials name and elastic constants, as well as a list of properties to be tabulated. A simple input file is given in [Ex. 6](#). The `database` keyword triggers the database mode and is followed by the database file name. The `data_prop` keyword is followed (on the same line) by the number of properties to appear in the output, and the next line contains their codes. The codes list is detailed in [Appendix B](#). In this example, the minimum and maximum of Young's modulus, linear compressibility, Poisson's ratio, as well as the bulk compressibility (inverse of bulk modulus) are requested.

The syntax of the database file is simple and is illustrated in [Ex. 7](#). Each line contains first a identifier, then the type of data (C if stiffnesses, S if compliances), followed by a symmetry code and finally by the data (following the order convention in [Appendix A](#)). Anything after the last elastic constant will be ignored by the program, but can be used for comments or references. The last line must be `stop`.

EIAM has no sorting or parsing facilities, and the entirety of a database will be treated, which can take some time. We advise the user to keep their master database in a spreadsheet format to benefit from superior editing and sorting capabilities, and to export the relevant section in a text file when required.

Please note that the default value for the θ, ϕ grid is used (24, 24). If increased accuracy is desirable, `thet` and `phi` can still be used.

4.7. Case study 3: negative linear compressibility

In a pioneering article [\[3\]](#), Baughman and coworkers used a primitive methodology to scan a database of known elastic constants in order to identify those materials which exhibit negative linear compressibility. Out of around five hundred compounds, they suggested that thirteen did show negative linear compressibility: two trigonal, two tetragonal, six orthorhombic and three monoclinic, but no triclinic. The procedure was strangely indirect and consisted in looking for linear compressibility that exceeds the bulk compressibility (sign of negative area compressibility in the perpendicular plane). The reasons for this choice are not clear, one can only postulate that as this method samples a full plane for the cost of one direction, it is efficient if only the principal axes are investigated (which is implied, but never spelt

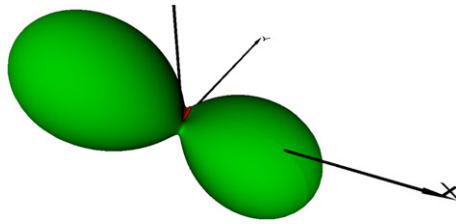


Fig. 8. 3D representation of linear compressibility for ammonium tetraoxalate dihydrate. (For interpretation of the references to colour in this figure legend, the reader is referred to the web version of this article.)

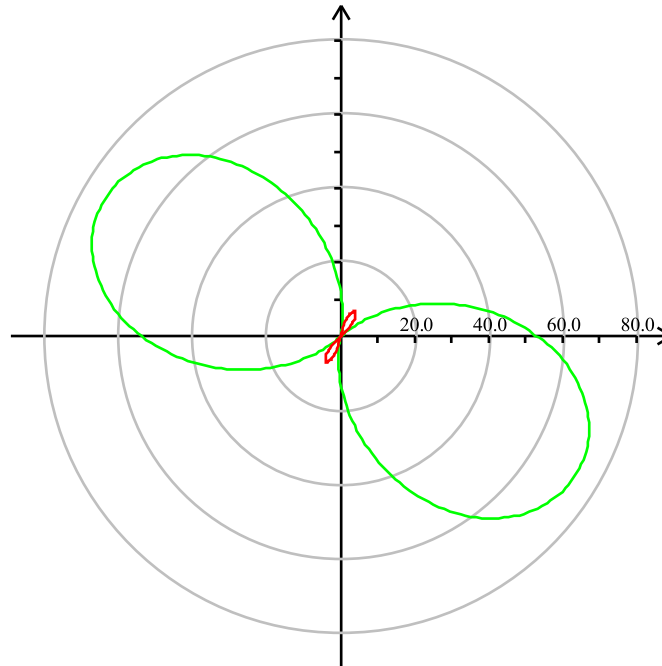


Fig. 9. 2D representation of linear compressibility for ammonium tetraoxalate dihydrate in the x - z plane. (For interpretation of the references to colour in this figure legend, the reader is referred to the web version of this article.)

out in the article). We use EIAM to re-examine the data, with a full directional scan. We focus on the lower symmetry crystals, and show that out of six triclinic crystals present in the Landolt-Börnstein tables, two do clearly show negative linear compressibility: ammonium tetraoxalate dihydrate and potassium tetraoxalate dihydrate. These compounds had been missed by the computationally simpler but less complete previous methodology. The linear compressibility for ammonium tetraoxalate dihydrate is shown in 3D and 2D in Figs. 8 and 9.

4.8. Case study 4: anisotropy measures

The original motivation for (and reason for the acronym of) EIAM's precursor was in fact an article by Ledbetter and Migliori [20] describing an extension to Zener's anisotropy measure [21]. They describe a straightforward method where the anisotropy is described by the ratio of maximum transverse sound velocity to minimum transverse sound velocity (called A^*), which corresponds to the Zener measure for cubic crystals (ratio of shear moduli),

$$A^* = \frac{v_{\min}^2}{v_{\max}^2}. \quad (18)$$

But what is meant by elastic anisotropy? The Ledbetter definition is attractive for historical reasons as it links well with the Zener ratio, but also because it is of relevance in the field of geosciences, where transverse wave velocities in different rock layers help locating or predicting earthquakes [22] for instance.

Other measures of anisotropy also suggests themselves, for instance a ratio of maximum and minimum of Young's or shear modulus. Are these measures correlated and does "elastic anisotropy" means anything in the absence of reference to a given property? A recent paper by Ranganathan and Ostojia-Starzewski [23] argues it does, and they propose a anisotropy measure based on the Reuss and Voigt averages,

$$A_u = 5 \frac{G^V}{G^R} + \frac{K^V}{K^R} - 6. \quad (19)$$

They also compare this measure with A^* , but their analysis is weakened by their inability to compute A^* for low symmetry crystal systems. As the analytical mathematical derivations are feasible for the higher symmetry crystal systems, but are very difficult for hexagonal onwards, the database capabilities of EIAM provide a superior way to investigate the topic of elastic anisotropy. This general problem

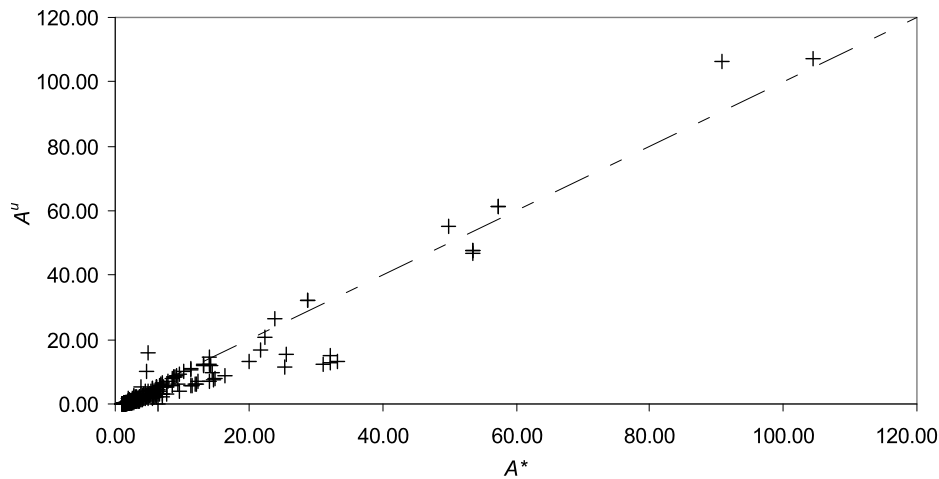


Fig. 10. Comparison of recent elastic anisotropy measures A^u and A^* .

goes beyond the scope of this article, but to demonstrate ELAM capabilities we plot A^u vs A^* for 438 crystals, of all 7 crystal systems. Fig. 10 demonstrates that these two measures are in general agreement, even for low symmetry crystal systems.

5. Conclusion

In this paper we have detailed the Fortran90 code, ELAM, for manipulation and representation of elastic properties of anisotropic frameworks (chiefly crystals). We have presented the required elements of theory of elasticity, and the conventions for 3D representation. We have also given detailed installation and execution notes. The operations of the codes have been illustrated by examples of increasing complexity, but also of direct relevance to contemporary problems: direction for extreme values of elastic properties, identification of materials exhibiting extreme properties and elastic anisotropy.

Acknowledgement

AM acknowledges the support of EPSRC, through grant EP/G064601/1.

Appendix A. List of keywords/options

Keywords are either stand alone (SA), require data on the following line(s) (FL), or must be accompanied by an integer on the same line AND data on following lines (I + FL)

A.1. Generic keywords

Keyword	Use	Default
titl	FL, title of the study, only appears in .log file	"
outpu	FL, root name for output files	'ELAM'
verbose	SA, triggers verbose mode and outputs too much information in .log	False
stiff	SA, elastic constants are read as components of stiffness matrix	True
compli	SA, elastic constants are read as components of compliance matrix	False
thet	FL, number of steps of angle theta (Fig. 2) for which properties are calculated	24
phi	FL, as above, for phi	24
cubi	FL, 3 elastic constants for cubic crystal system (C_{11} , C_{44} , C_{12})	N/A
hexa	FL, 5 elastic constants for hexagonal crystal system (C_{11} , C_{33} , C_{44} , C_{12} , C_{13})	N/A
tetr	FL, 7 elastic constants for tetragonal crystal system (C_{11} , C_{33} , C_{44} , C_{66} , C_{12} , C_{13} , C_{16})	N/A
trig	FL, 7 elastic constants for trigonal crystal system (C_{11} , C_{33} , C_{44} , C_{12} , C_{13} , C_{14} , C_{15})	N/A
orth	FL, 9 elastic constants for orthorhombic crystal system (C_{11} , C_{22} , C_{33} , C_{44} , C_{55} , C_{66} , C_{12} , C_{13} , C_{23})	N/A
mono	FL, 13 elastic constants for monoclinic crystal system (C_{11} , C_{22} , C_{33} , C_{44} , C_{55} , C_{66} , C_{12} , C_{13} , C_{23} , C_{15} , C_{25} , C_{35} , C_{46})	N/A
tric	FL, 21 elastic constants for triclinic crystal system (C_{11} , C_{12} , C_{13} , C_{14} , C_{15} , C_{16} , C_{22} , C_{23} , C_{24} , C_{25} , C_{26} , C_{33} , C_{34} , C_{35} , C_{36} , C_{44} , C_{45} , C_{46} , C_{55} , C_{56} , C_{66})	N/A
C	FL, stiffness matrix, 6 lines of 6 coordinates	N/A
S	FL, compliance matrix, 6 lines of 6 coordinates	N/A
database	SA, Triggers database mode	False
data_prop	FL, list of output codes (Appendix B)	N/A
stop	Last line of input	N/A

A.2. 3D keywords

Keyword	Use	Default
young	SA, generates a 3d representation of Young's modulus	False
shear	SA, as above, for Shear ratio	False
compress	SA, as above, for linear compressibility	False
poisson	SA, as above, for Poisson's ratio	False
sound	SA, as above, for sound velocities	False
3dth	FL, number of steps of angle theta for which properties are represented	12
3dph	As above, see Figs. 2 and 3	12
3daxes	SA, includes XYZ axes in 3D files	False
color_bg	FL, 3 colour code (RBG), background colour	(0 0 0)
color_front	FL, 3 colour code, foreground colour	(1 1 1)
color_pos	FL, 4 colour code (RBG+transparency), for positive values of non-optimised elastic properties (Young's modulus, compressibility)	(0 .8 0 0)
color_neg	As above, for negative values	(.8 0 0 0)
color_max	FL, 4 colour code, for maximum values of complex elastic properties	(0 0 .8 .5)
color_minp	As above, but for minimum positive	(.8 0 0 0)
color_minn	As above, but for minimum negative	(0 .8 0 0)
color_avep	As above, but for average positive	(0 0 0 1)
color_aven	As above, but for average negative	(0 0 0 1)

A.3. 2D keywords

Keyword	Use	Default
plane_xy	FL, 3 coordinates of a vector, select the plane in which a 2D cut is preformed (plane perpendicular to coordinates)	N/A
plane_an	As above, but vector described by θ and ϕ	N/A
2dyoung	SA, a postscript plot of Young's modulus in the chosen plane will be created	False
2dyoung_tick	FL, tick marks interval, output marks on axes of Young's modulus plot	0
2dyoung_circ	FL, circles interval, output circles on Young's modulus plot	0
2dyoung_scale	FL, scale interval, output scale on axes of Young's modulus plot	0
2dshear	SA, a postscript plot of the shear modulus in the chosen plane will be created	False
2dshear_tick,	As the 2dyoung_equivalents	0
2dshear_circ,		
2dshear_scale		
2dcomp	SA, a postscript plot of the linear compressibility in the chosen plane will be created	False
2dcomp_tick,	As the 2dyoung_equivalents	0
2dcomp_circ,		
2dcomp_scale		
2dpois	SA, a postscript plot of Poisson's ratio in the chosen plane will be created	False
2dpois_tick,	As the 2dyoung_equivalents	0
2dpois_circ,		
2dpois_scale		
2dsound	SA, a postscript plot of the sound velocities in the chosen plane will be created	False
2dsound_tick,	As the 2dyoung_equivalents	0
2dsound_circ,		
2dsound_scale		
2dtitlex	FL, character string, title of X axis	"
2dtitley	FL, character string, title of Y axis	"

Appendix B. Elastic property codes

The property codes used in the database modes range from 1 to 999. With few exceptions, they consist of a three figure code. The first number refers to the property itself, as in [Table B.1](#).

The second two numbers refine the definition, see [Table B.2](#).

The leading 0 must be omitted for the stiffnesses and compliances. Codes 1 to 21 comprise the stiffnesses in order 11, ... 16, 22, ... 26, ... 66. Codes 51 to 1 are the equivalent for the compliances.

Table B.1

First figure code definition, for a code of the form Xnn.

X = 0	X = 1	X = 2	X = 3	X = 4	X = 5
Stiffnesses or compliances	Young's modulus	Shear modulus	Compressibility	Poisson's ratio	Sound velocity

Table B.2

Second part code definition, for a code of the form Xnn.

nn = 00 Direct average	nn = 01 Reuss average	nn = 02 Voigt average	nn = 03 Hill average	nn = 04 Bulk compressibility (only 304)
nn = 10 minimum (X = 5: minimum transverse)	nn = 11 nn = 12 direction of minimum: θ, ϕ	nn = 13 nn = 14 nn = 15 direction of minimum: x, y, z		nn = 16 nn = 17 nn = 18 Miller indices for minimum
nn = 20 maximum (X = 5: maximum transverse)	nn = 21 nn = 22 direction of maximum: θ, ϕ	nn = 23 nn = 24 nn = 25 direction of maximum: x, y, z		nn = 26 nn = 27 nn = 28 Miller indices for maximum
nn = 30 X = 5 only: longitudinal		nn = 33 nn = 34 nn = 35 transverse direction at minimum (vector b): x, y, z (only for X = 2 or 4)		nn = 36 nn = 37 nn = 38 transverse direction at minimum (vector b): Miller indices (only for X = 2 or 4)
		nn = 43 nn = 44 nn = 45 transverse direction at maximum (vector b): x, y, z (only for X = 2 or 4)		nn = 46 nn = 47 nn = 48 transverse direction at maximum (vector b): Miller indices (only for X = 2 or 4)

References

- [1] R. Lakes, Science 235 (1987) 1038.
- [2] R.H. Baughman, J.M. Shacklette, A.A. Zakhidov, et al., Nature 392 (1998) 362.
- [3] R.H. Baughman, S. Stafstrom, C.X. Cui, et al., Science 279 (1998) 1522.
- [4] C.N. Weng, K.T. Wang, T. Chen, Advances in Fracture and Materials Behavior 1, 2 (33–37) (2008) 807.
- [5] G.D. Barrera, J.A.O. Bruno, T.H.K. Barron, et al., Journal of Physics – Condensed Matter 17 (2005) R217.
- [6] U.F. Kocks, C.N. Tomé, H.-R. Wenk, Texture and Anisotropy: Preferred Orientations in Polycrystals and Their Effect on Materials Properties, Cambridge University Press, Cambridge, 2000.
- [7] A. Cazzani, M. Rovati, International Journal of Solids and Structures 40 (2003) 1713.
- [8] A.G. Every, A.K. McCurdy, in: Landolt-Börnstein (Ed.), Numerical Data and Functional Relationships in Science and Technology, vol. 29a, Springer Verlag, Berlin, 1993.
- [9] G. Simmons, H. Wang, Single Crystal Elastic Constants and Calculated Aggregate Properties: A Handbook, MIT Press, Cambridge, 1971.
- [10] J.F. Nye, Physical Properties of Crystals, Clarendon Press, Oxford, 1985.
- [11] T.C.T. Ting, Anisotropic Elasticity, Oxford University Press, New York, 1996.
- [12] M.T. Dove, Introduction to Lattice Dynamics, Cambridge University Press, Cambridge, 1993.
- [13] W. Voigt, Teuber, Leipzig, 1928, p. 962.
- [14] A. Reuss, Z. Angew. Math. Mech. 9 (1929) 55.
- [15] R. Hill, Proceedings of the Physical Society of London Section A 65 (1952) 349.
- [16] J. Kopp, International Journal of Modern Physics C 19 (2008) 845.
- [17] T. Pang, An Introduction to Computational Physics, Cambridge University Press, Cambridge, 1997.
- [18] T.C.T. Ting, T.Y. Chen, Quarterly Journal of Mechanics and Applied Mathematics 58 (2005) 73.
- [19] A.N. Norris, Proceedings of the Royal Society A – Mathematical Physical and Engineering Sciences 462 (2006) 3385.
- [20] H. Ledbetter, A. Migliori, Journal of Applied Physics 100 (2006) 063516.
- [21] C. Zener, Elasticity and Anelasticity of Metals, University of Chicago Press, Chicago, 1948.
- [22] A.B. Belonoshko, N.V. Skorodumova, A. Rosengren, et al., Science 319 (2008) 797.
- [23] S.I. Ranganathan, M. Ostoja-Starzewski, Physical Review Letters 101 (2008).